THE JOURNAL OF BIOLOGICAL CHEMISTRY VOL. 281, NO. 20, pp. 13894–13898, May 19, 2006

Only One Protomer Is Active in the Dimer of SARS 3C-like Proteinase*[S]

Received for publication, October 3, 2005, and in revised form, March 8, 2006 Published, JBC Papers in Press, March 24, 2006, DOI 10.1074/jbc.M510745200

Hao Chen[‡§1], **Ping Wei**[‡1], **Changkang Huang**[‡], **Lei Tan**[‡], **Ying Liu**[‡], **and Luhua Lai**[‡§2]

From the [‡]*State Key Laboratory for Structural Chemistry of Unstable and Stable Species, College of Chemistry, Peking University, Beijing 100871, China and* [§]*Center for Theoretical Biology, Peking University, Beijing 100871, China*

The severe acute respiratory syndrome coronavirus 3C-like protease has been proposed to be a key target for structurally based drug design against SARS. The enzyme exists as a mixture of dimer and monomer, and only the dimer was considered to be active. In this report, we have investigated, using molecular dynamics simulation and mutational studies, the problems as to why only the dimer is active and whether both of the two protomers in the dimer are active. The molecular dynamics simulations show that the monomers are always inactive, that the two protomers in the dimer are asymmetric, and that only one protomer is active at a time. The enzyme activity of the hybrid severe acute respiratory syndrome coronavirus 3C-like protease of the wild-type protein and the inactive mutant proves that the dimerization is important for enzyme activity and only one active protomer in the dimer is enough for the catalysis. Our simulations also show that the right conformation for catalysis in one protomer can be induced upon dimer formation. These results suggest that the enzyme may follow the association, activation, catalysis, and dissociation mechanism for activity control.

In early 2003, a highly epidemic disease named severe acute respiratory syndrome (SARS)[3] first broke out in China and then quickly spread to other circumjacent countries (1). Research proved that the nosogenesis was a novel coronavirus. In the coronavirus life cycle, 3C-like proteinase ($3CL^{pro}$) is important and indispensable and is a pivotal target in anti-SARS drug design (2).

SARS $3CL^{pro}$ shares 40 and 44% sequence identity to $3CL^{pro}$ of human coronaviruses 229E and transmissible gastroenteritis virus, the crystal structures of which have been resolved (2, 3). Several homology models for SARS $3CL^{pro}$ have been reported (2, 4, 5). More recently, the crystal structures of the enzyme and the inhibitor-enzyme complex have been determined (6–11). All structures are very similar and consist of three domains. The first two domains form a chymotrypsin fold, and the third domain is an extra helix domain that plays an important role in dimerization and enzyme activity (12). All of the proteins are dimeric in the crystal structures, and there exists an equilibrium between the monomer and dimer in solution. In our previous work, we have observed that the activity increases with the increase of enzyme concentration, indicating the dimer is the active form of the proteinase (13). Other groups have studied the function of the N-finger in dimerization and enzyme activity. The N-terminal residues 1–5 delete transmissible gastroenteritis virus $3CL^{pro}$, and the N-terminal residues 1–7 delete SARS $3CL^{pro}$; both have been reported to have no enzyme activities (3, 14–16). Interestingly, Chen *et al.* (14) report that the N-finger deletion mutation does not affect the dimerization of SARS $3CL^{pro}$. Contrary to this, Hsu *et al.* (16) has found that the N-4 truncated protease is mainly monomeric and has little enzyme activity, but the N-3 truncated protease is almost the same as the wild-type enzyme. Furthermore, Chou *et al.* (17) report that the mutation of R4A, E290A, and R4A/E290A weakens the dimerization.

All current experimental evidence agrees that only the dimeric form of proteinase is active. But why the monomer is inactive remains unclear. The other intriguing problem is whether the two protomers in one dimer are both active at the same time, whether only one protomer is active, or whether the two protomers are alternately active at different times. We have used molecular dynamics simulations and hybrid protein experiments to address these problems. Simulations on the dimer and two monomers were done. Our analysis confirms that the monomers are always inactive and that the two protomers in the dimer are asymmetric with probably only one protomer active at one time. We also purposely made a hybrid protein dimer of the wild-type protein and the inactive C145A mutant and measured its enzyme activity. The hybrid protein was shown to be active. This experiment strongly supports that dimerization is essential for enzyme activity and only one active protomer in the dimer is enough for the catalysis.

EXPERIMENTAL PROCEDURES

Molecular Dynamics Simulation—The molecular dynamics simulations were performed using the GROMACS software package version 3.2.1 (18, 19) with the OPLS/AA force field (20). The initial conformations of the dimer (model 1) and monomers (models 2 and 3) all came from the x-ray crystal structure of SARS $3CL^{pro}$ at pH 8.0 (Protein Data Bank (PDB) code 1uk2; resolution 2.2 Å) (6). Because the two protomers in the crystal structure were asymmetric (r.m.s.d. of heavy atoms was 1.38 Å), the two protomers were calculated separately (model 2 was from the protomer A of the crystal structure, also named as protomer A^M in the following analysis; model 3 was from the protomer B, also named as protomer B^M; accordingly, the protomers A and B in model 1 were respectively named protomers A^D and B^D). These three models were simulated in a TIP4P (21) water environment. The model systems were rectangular periodic boxes, and the minimum distance between the protein and box boundary was >0.90 nm. To neutralize the charges and simulate a real physiological environment, some water molecules were replaced by Na^+ and Cl^- ions. In the final models, model 1 had 20,373 water molecules, 63 Na^+ ions, and 57 Cl^- ions in a $7.9 \times 9.58 \times 9.52$ nm^3 box; model 2 had 10,003 water molecules, 31 Na^+ ions, and 28 Cl^- ions in a $5.55 \times 9.58 \times 6.57$ nm^3 box; and model

* This work was supported in part by the Ministry of Science and Technology of China and National Natural Science Foundation of China (20473001, 90403001, 30490245, 20228306). The costs of publication of this article were defrayed in part by the payment of page charges. This article must therefore be hereby marked "*advertisement*" in accordance with 18 U.S.C. Section 1734 solely to indicate this fact.

[S] The on-line version of this article (available at http://www.jbc.org) contains supplemental Figs. S1 and S2 and Tables SI and SII.

[1] Both authors contributed equally to this work.

[2] To whom correspondence should be addressed: College of Chemistry and Molecular Engineering, Peking University, Beijing 100871, China. Tel.: 86-10-62757486; Fax. 86-10-62751725; E-mail: lhlai@pku.edu.cn.

[3] The abbreviations used are: SARS, severe acute respiratory syndrome; $3CL^{pro}$, 3C-like proteinase; r.m.s.d., root mean square deviation.

3 had 9,858 water molecules, 31 Na^+ ions and 28 Cl^- ions in a $5.53 \times 6.73 \times 9.52$ nm^3 box.

All simulations were under a constant pressure and temperature ensemble using the Nose-Hoover method (22) for temperature control and the Parrinello-Rahman method (23) for pressure control. Van der Waals interactions were computed using a twin range cutoff method, and electrostatic interactions were computed using the particle-mesh Ewald method (24). All bonds with hydrogen atoms were constrained by the LINCS algorithm (25). Before simulation, all three systems were minimized with the steepest descent algorithm. During simulations, the time step was set to 1.0 fs, and conformations were saved every 10 ps. Thereafter, four 10-ns simulations were run for each system. Furthermore, to investigate the conformation exchange between the two protomers, we built two pseudodimers. Pseudodimer A was built with two protomers A of the crystal structure, whereas pseudodimer B was built with two protomers B. Subsequently, the four simulations were run for 5 ns for pseudodimer A and 2 ns for pseudodimer B, respectively. All simulations were performed at 310 K in 1 atmosphere, and the total of the simulation time for all trajectories was 148 ns.

Calculation of Substrate Binding Energy—The model substrate was built into the trajectories, and the energies were calculated in the CHARMM19 force field (26) using the CHARMM software package (27). The sequence of the model peptide was TSAVLQ, which was the N-terminal P6-P1 sequence of a reported best peptide substrate (13). The initial conformation and the relative geometric position of the enzyme and the substrate were derived from the x-ray crystal structure (PDB code 1uk4; chain G). We then fixed the enzyme conformation and optimized the complex. During the conformation optimization, the distances of the following important atom-atom pairs had been harmonically constrained, namely Cys^{145} SG-Gln^6 C, Glu^{166} OE1-Gln^6 NE2, His^{163} NE2-Gln^6 OE1, Glu^{166} O-Val^4 N, and Glu^{166} N-Val^4 N.

Site-directed Mutagenesis of SARS 3CL^{pro}—The C145A mutant of SARS $3CL^{pro}$ was prepared with the QuikChange site-directed mutagenesis kit (Stratagene) using pET 3CLP-21h (28) as a template. The mutation was verified by nucleotide sequencing.

The Expression and Purification of SARS 3CL^{pro}—The wild-type and mutational SARS $3CL^{pro}$ were expressed and purified as described in our previous report (29). The purity was verified by SDS-PAGE to be >95%. The enzyme concentration was calculated from absorbance at 280 nm with 1.04 mg/optical density.

Colorimetric Enzyme Assay for the Wild-type and the Hybrid Protein—The enzyme activity was measured by a colorimetric assay as reported previously (28). In short, 20 μl of pNA substrate stock solution (2 mM Thr-Ser-Ala-Val-Leu-Gln-pNA water solution) was added to 180 μl of 25 °C preheated reaction buffer (40 mM phosphate-buffered saline, 1 mM EDTA, 0.2 mg/ml bovine serum albumin, 3 mM dithiothreitol, pH 7.3), which contained SARS $3CL^{pro}$ wild-type enzyme and the C145A mutant. The concentration of wild-type enzyme was held at either 0.6 or 0.8 μM, and the concentration of C145A was changed from 2.5 to 500 μM. Colorimetric measurements of enzymatic activity were performed in 96-well microtiter plates using a multiwell ultraviolet spectrometer (Spectra Max 190, Molecular Devices) at 390 nm. Each assay was repeated twice. We also determined the wild-type proteinase activity at nine concentrations from 0.1 to 3 μM alone or with a high concentration of C145A mutant protein.

RESULTS

Dynamics of the Dimer and Monomers—To find out the differences between the dimer and the monomer, molecular dynamics simulations were performed. For all trajectories, r.m.s.d. values of all heavy atoms were calculated. After 2 ns, all of the three systems were approximately in equilibrium (supplemental Fig. S1). In the following analysis, only the last 8 ns in each trajectory were checked for all of the 12 trajectories.

TABLE 1
Number of hydrogen bonds between Cys-145 SG and His-41 ND1/NE2

	1[a]	2[a]	3[a]	4[a]	Total
Protomer A^D	428	15	0	303	746
Protomer B^D	44	176	203	13	436
Protomer A^M	3	0	0	0	3
Protomer B^M	334	33	434	356	1,157

[a] The numbers 1, 2, 3, and 4 represent the four trajectories for each system.

The Conformation of Catalytic Dyad—We have shown that SARS $3CL^{pro}$ underwent a general serine protease catalysis mechanism, and His^{41} and Cys^{145} comprised the catalytic dyad (28). The number of occurrences of the right conformation for the dyad was counted in all trajectories. Here the right conformation meant that the SG atoms in Cys^{145} and the ND1/NE2 atom in His^{41} forms a hydrogen bond as recognized by HBPLUS (30). The results were summarized in Table 1. The dyad have chances to be in the right catalytic conformation in protomer A^D, protomer B^D and protomer B^M, whereas no suitable conformation for catalysis was found in all four trajectories of protomer A^M.

The Conformation of the Substrate Binding Pocket—Combining the analysis of transmissible gastroenteritis virus $3CL^{pro}$ by Anand *et al.* (3) and of SARS $3CL^{pro}$ (6) by Yang *et al.* (6), we summarize the following key structure elements for catalysis as follows: 1) the oxyanion hole, 2) Y-*X*-H motif, 3) the hydrophobic packing of His^{163} and Phe^{140}, and 4) conformations around Glu^{166}. All of these features were checked in the simulations. For the crystal structure, protomer A passed all four tests, and protomer B failed in tests 1 and 4 (6).

Oxyanion Hole—The distances between the main chain oxygen atom of the Gln residue at the P1 position of the substrate and the main chain amides of Gly^{143}, Ser^{144}, and Cys^{145} were calculated. The coordinates of the substrate came from the modeling result in the later section. When all three distances were <4.5 Å, we defined it as a good oxyanion hole. The results were listed in supplemental Table SI. Protomers A and B behaved quite differently. Both in the dimer and in stand-alone monomer, protomer B was always bad and protomer A was always good.

Tyr-Xaa-His Motif—The hydrogen bond of Tyr^{161} OH and His^{163} ND1 is listed in supplemental Table SII. The results indicated that the Y-*X*-H motif was much more stable in protomer A than in protomer B, both in the dimer and in the monomer.

Hydrophobic Packing between His^{163} and Phe^{140}—The centroid distance and the cosine of the dihedral angle between the imidazole ring of His^{163} and the phenyl ring of Phe^{140} were monitored. Here the angle was the dihedral angle between the plane that was defined by atoms CG, ND1, and NE2 in the imidazole ring of His^{163} and the plane that was defined by atoms CG, CE1, and CE2 in the phenyl ring of Phe^{140}. The results were shown in supplemental Fig. S2, *A* and *B*. The hydrophobic packing between His^{163} and Phe^{140} in protomer A was much better than that in protomer B.

Conformation around Glu^{166}—The hydrogen bond of Glu^{166} OE1/OE2 was also monitored and listed in supplemental Table SII. In the monomers, it can form a hydrogen bond with His^{163} (in protomer A^M) or Asn^{142} (in protomer B^M) from the same protomer. Both interactions block the binding of substrate.

Furthermore, we also monitored the hydrogen bond of the atoms around the active sites and the binding pocket along the trajectories. These atoms include Cys^{145} SG, His^{41} NE2/ND1, Gly^{143} O, Tyr^{126} OH, Asp^{187} OD1/OD2, and Arg^4 O/N. The results were also listed in supplemental Table SII. We noticed that the hydrogen bonds of Gly^{143}

TABLE 2
Substrate binding to the dimer and the monomer

		Vdw[a]	Elec[b]	Inner[c]
			kcal/mol	
The full substrate				
DIMER	Protomer A^D	−15.57	−890.00	132.64
	Protomer B^D	−4.34	−860.44	162.96
MONO	Protomer A^D	−6.60	−850.55	134.96
	Protomer B^D	−4.45	−828.80	128.93
P1 position of substrate				
DIMER	Protomer A^D	−5.04	−253.85	39.87
	Protomer B^D	−0.42	−217.21	52.28
MONO	Protomer A^D	−1.82	−219.83	40.20
	Protomer B^D	4.17	−208.58	41.82

[a] The van der Waals energy between the substrate and the enzyme.
[b] The electrostatic energy between the substrate and the enzyme.
[c] The internal energy of the substrate.

O–Asn[28] ND2 and Ser[139] N–Tyr[126] OH were very stable in protomer A but disappeared or were less stable in protomer B. We also noticed that, at the dimeric interface, Ser[139] OG of protomer A can form a stable hydrogen bond with the main chain of Arg[4] in protomer B, whereas Ser[139] OG of protomer B cannot.

Binding of Substrate to the Dimer and Monomers—We built the model substrate into the trajectories and calculated the binding energies. The results were summarized in Table 2. The median of the van der Waals interaction energy in the P1 pocket for the two protomers in the dimer and the two monomers were −5.04, −0.42, −1.82, and 4.17 kcal/mol, respectively. It is clear that protomer A^D has much stronger binding ability than all of the others.

Conformation Transition between Protomers A and B—To see whether protomers A and B in the dimer can exchange conformation, two additional simulations were done. Thereafter, the r.m.s.d. values of the binding pocket between the trajectories and the protomer A of the crystal structure were calculated and summarized in Table 3. Here the binding pocket was defined by residues 41, 140, 142–145, 161, 163, 166, and 172. In pseudodimer A, we noticed that only one protomer could stay in the original conformation. For example, in trajectory 1, the average r.m.s.d. values of two protomers were 1.41 and 2.06 Å (Fig. 1*A*). In pseudodimer B, we observed a clear transition; in trajectory 3, the average r.m.s.d. value of one protomer was lowered to 1.47 from 1.95 Å (Fig. 1*B*). This means that proper conformation for catalysis can be induced by dimer formation.

Enzymatic Activity of the Wild-type and the Hybrid SARS $3CL^{pro}$—In the previous study, we have reported that the active site mutation C145A gave an inactive enzyme (28). The mutant did not show any visible enzyme activity at concentrations as high as 100 μM. However, when it was added into the low concentration solution of the wild-type enzyme (protein was partly in monomeric form), the resulting hybrid enzyme exhibited increased activity (Fig. 2*A*). Along with the concentration increase of C145A, the apparent activity of the hybrid protein reached a maximum value. As a control, no visible change in activity was observed when different concentrations of bovine serum albumin were added (Fig. 2*A*).

Furthermore, we tried to analyze the activity quantitatively. For the wild-type proteinase alone, there is an equilibrium between the monomer and dimer, and the enzyme activity comes from the dimer. Therefore, we used the following equations.

$$K_d = [M][M]/[D] \quad \text{(Eq. 1)}$$

$$[M] + 2[D] = C_T \quad \text{(Eq. 2)}$$

Here [M], [D], and C_T were the enzyme concentrations of the monomer, the dimer, and the total concentration calculated as the monomer, and K_d was the apparent dissociation constant of the dimer. Fitting the data at different C_T values using Equation 3 by Origin version 6.0 (OriginLab), the k_{cat} was calculated to be ~3.34 min^{-1}, and the K_d was ~0.81 μM (Fig. 2*B*).

$$V_{max} = k_{cat}[D] = k_{cat}\frac{K_d + 4C_T - \sqrt{K_d^2 + 8K_dC_T}}{8} \quad \text{(Eq. 3)}$$

For the hybrid proteinase, because C145A was in excess, all of the wild-type protomers could form the hybrid dimer. As Fig. 2*B* shows, a perfect linear relationship was detected between the enzyme activity and the concentration of the hybrid dimer (with a correlation coefficient of 0.9995, going through the origin). After data fitting, the k_{cat} of the hybrid dimer was calculated to be ~ 1.58 min^{-1}.

TABLE 3
Average r.m.s.d. value (Å) of the binding pocket between trajectories and protomer A of the crystal structure
The binding pocket was defined by residues 41, 140, 142–145, 161, 163, 166, and 172. For the pseudo dimers A and B, only the last nanosecond of each simulation was calculated.

	1	2	3	4
Protomer A^D	1.46	1.43	1.90	1.61
Protomer B^D	2.48	2.38	2.40	2.43
Protomer A^D in the pseudo dimer A	1.41	1.85	1.70	1.93
Protomer B^D in the pseudo dimer A	2.06	1.48	1.50	1.55
Protomer A^D in the pseudo dimer B	2.82	2.15	2.04	2.26
Protomer B^D in the pseudo dimer B	2.14	2.06	1.47	2.18

DISCUSSION

Difference between the Dimer and Monomers in Simulations—To reveal the differences between the dimer and the monomers, the total of the molecular dynamics simulations for the dimer and monomers run under physiological conditions was 148 ns. Thereafter, key structure features necessary for catalysis were checked. Similar to the previous analysis based on the crystal structure (6), protomer B^D was also found to be unsuited for catalysis in our simulations. Moreover, we found that some structure features required by catalysis were destroyed in protomer A^M, such as 1) no suitable conformation for catalytic dyad and 2) Glu[166] forming a hydrogen bond with His[163] and blocking the substrate binding. By the conformation analysis of the trajectories, two binding-related hydrogen bonds, which behaved very differently between protomers A and B, were found. Furthermore, the binding energy of the model substrate with the enzyme also shows that protomer A^D has much stronger binding ability than protomer B^D and the two stand-alone monomers.

Dimerization and Enzyme Activity—After the above analysis, we now have an overview about the dimerization and enzyme activity. In the dimer, only protomer A is active and protomer B can help protomer A maintain the correct catalytic conformation. However, exactly how protomer B makes protomer A stable in the correct conformation for catalysis is still unclear. Anand *et al.* (3) ascribed it to the hydrogen bond of Glu[166] OE1/OE2 and Ser[1] N in the other protomer, and recently Tan *et al.* (10) ascribed it to the hydrogen bond between the N terminus of the other protomer and the main chain of Phe[140]. However, the mutation experiment showed that the N-3 truncated protease was also active and remained dimeric (16). In our simulations, we noticed that, in the dimeric interface, hydrogen bond S139A OG–A4B O/N was stable, whereas S139B OG–A4A O/N did not exist. The mutation experiment also showed that the N-4 truncated protease was inactive (16). Therefore, this interaction was probably also very important. Furthermore, the stabilization may only depend on the dynamic behavior of the whole structure.

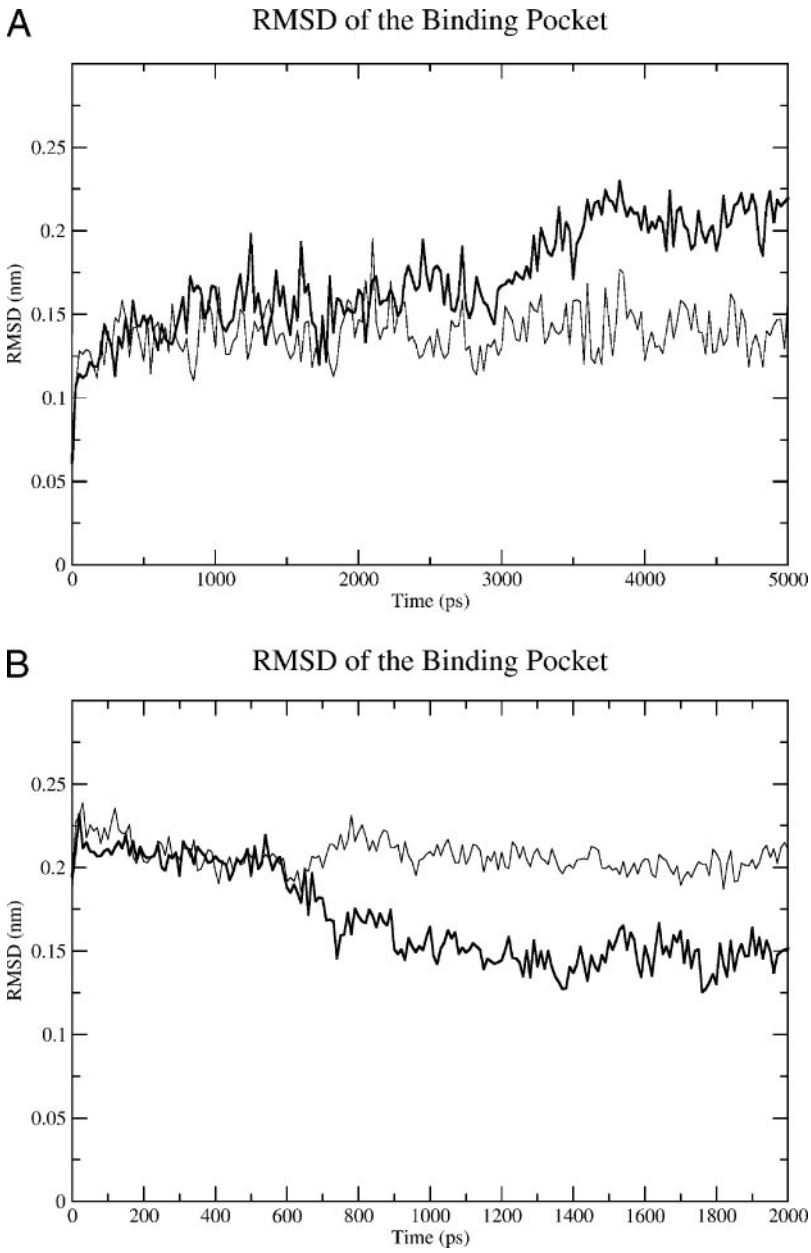

FIGURE 1. **The r.m.s.d. values of the binding pocket in two typical trajectories.** Shown are the heavy atom r.m.s.d. values of the binding pocket in trajectories fitted to the conformation of protomer A in the crystal structure (PDB code 1uk2). Here the binding pocket was defined by residues 41, 140, 142–145, 161, 163, 166, and 172. *A*, the trajectory 1 in the pseudodimer A simulation. *B*, the trajectory 3 in the pseudodimer B simulation.

Moreover, we measured the enzyme activity of the hybrid SARS $3CL^{pro}$. The experiments showed that the enzyme activity increased dramatically by adding the inactive mutant C145A. This proved two things. 1) C145A could form the hybrid dimer with the wild-type enzyme; otherwise the enzyme activity could not have been changed. 2) The hybrid dimer also had enzyme activity; otherwise along with the formation of the hybrid dimer, the enzyme activity would be decreased. Combining with our analysis from molecular dynamics simulations, we proposed that, in the hybrid dimer, the C145A monomer can perform the function of protomer B^D and help the wild-type enzyme protomer stay in the correct conformation. In conclusion, only one active protomer is required for the activity of the SARS $3CL^{pro}$ dimer. Furthermore, by the quantitative analysis under the enzyme assay condition, the apparent K_d was ~0.81 μM, which is much less than the K_d reported before for the pure enzyme (~14 μM) (29). It means that the substrate can stabilize the dimer, or in other words, the dimer has much stronger ability to bind the substrate than the monomer. The k_{cat} of the wild-type dimer and the hybrid dimer could also been deduced. It is interesting that the hybrid dimer has about one-half of the wild-type dimer activity. However, this phenomenon does not conflict with our previous conclusion. We concluded that only one protomer in the dimer was active at one time. For the pure wild-type enzyme dimer, there is always one protomer that stays in the active conformation. While in the hybrid dimer, the wild-type protomer may stay either in the active form or in the inactive form. Thus the hybrid dimer has only about one-half of the wild-type protein activity.

Conformation Transition between Protomers A and B—In the previous analysis, we found the two protomers in one dimer were asymmetric and only one protomer was active. Because the stand-alone monomer cannot maintain the active conformation, this asymmetry was because of dimerization. There are three possible mechanisms. 1) The two protomers in the dimer can exchange conformation. 2) During the association process of the two protomers, one becomes active and the other remains inactive. 3) A mixed mechanism of both items 1) and 2). In the simulations at normal body temperature, the conformational transition cannot be observed in our time scale. When we placed the two pro-

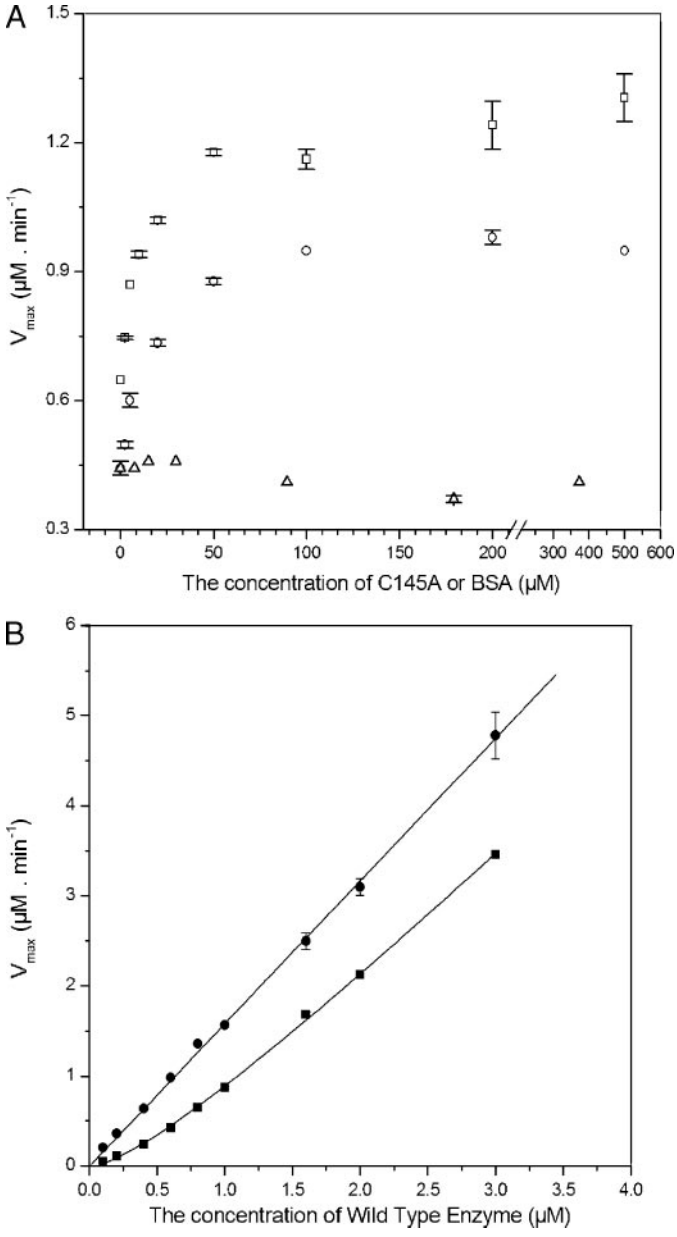

FIGURE 2. **The enzymatic activities of the hybrid SARS 3CL^{pro} and the wild-type enzyme.** *A* □, adding C145A into the wild-type enzyme of 0.8 μM; ○, adding C145A into the wild-type enzyme of 0.6 μM; △, adding bovine serum albumin into the wild-type enzyme of 0.6 μM as the control. The concentration of C145A or bovine serum albumin ranged from 2.5 to 500 μM. *B* ■, the wild-type enzyme concentration ranged from 0.1 to 3.0 μM; ●, the wild-type enzyme plus the high concentration C145A mutant (200 μM when C_{WT} ranged from 0.1 to 0.6 μM; 500 μM when C_{WT} ranged from 0.8 to 3.0 μM). All of the experiments were repeated two times.

tomers both in the inactive conformation (only after 2 ns), one conformational transition was observed in four simulations. This implies that mechanism 2 was the most possible one.

CONCLUSION

We have used molecular dynamics simulations and enzyme activity measurement of the hybrid protein to study why only the dimer of SARS 3CL^{pro} is active. Analysis of the simulation trajectories showed that stand-alone monomers cannot play the enzymatic role correctly, and only one protomer in the dimer is in the right state for catalysis. The experiments on the hybrid SARS 3CL^{pro} between the wild-type enzyme and the inactive mutant C145A revealed an increased enzyme activity. This supports that dimerization is important for the enzyme activity, and in the dimer, only one active protomer is enough for the catalysis. Furthermore, we studied the mechanism for activity control in the dimer. Our simulations show that the most probable mechanism is the right conformation, as catalysis can be induced upon dimer formation. As the dimer is relatively weak, the enzyme may follow the association, activation, catalysis, dissociation mechanism for activity control, and no conformational exchange is necessary within one dimer. Much more needs to be studied about why dimerization can induce and maintain the right conformation for catalysis. Our simulations and experiments confirm that dimerization was the essential requirement for enzyme activity and only one monomer is active in the dimer.

REFERENCES

1. Drosten, C., Gunther, S., Preiser, W., van der Werf, S., Brodt, H. R., Becker, S., Rabenau, H., Panning, M., Kolesnikova, L., Fouchier, R. A., Berger, A., Burguiere, A. M., Cinatl, J., Eickmann, M., Escriou, N., Grywna, K., Kramme, S., Manuguerra, J. C., Muller, S., Rickerts, V., Sturmer, M., Vieth, S., Klenk, H. D., Osterhaus, A. D., Schmitz, H., and Doerr, H. W. (2003) *N. Engl. J. Med.* **348,** 1967–1976
2. Anand, K., Ziebuhr, J., Wadhwani, P., Mesters, J. R., and Hilgenfeld, R. (2003) *Science* **300,** 1763–1767
3. Anand, K., Palm, G. J., Mesters, J. R., Siddell, S. G., Ziebuhr, J., and Hilgenfeld, R. (2002) *EMBO J.* **21,** 3213–3224
4. Xiong, B., Gui, C., Xu, X., Luo, C., Chen, J., Luo, H., Chen, L., Li, G., Sun, T., Yu, C., Yue, L., Duan, W., Shen, J., Qin, L., Shi, T., Li, Y., Chen, K., Luo, X., Shen, X., Shen, J., and Jiang, H. (2003) *Acta Pharmacol. Sin.* **24,** 497–504
5. Pang, Y.-P. (2004) *Proteins Struct. Funct. Bioinformat.* **57,** 747–757
6. Yang, H., Yang, M., Ding, Y., Liu, Y., Lou, Z., Zhou, Z., Sun, L., Mo, L., Ye, S., Pang, H., Gao, G., Anand, K., Bartlam, M., Hilgenfeld, R., and Rao, Z. (2003) *Proc. Natl. Acad. Sci. U. S. A.* **100,** 13190–13195
7. Hsu, M.-F., Kuo, C.-J., Chang, K.-T., Chang, H.-C., Chou, C.-C., Ko, T.-P., Shr, H.-L., Chang, G.-G., Wang, A. H.-J., and Liang. P.-H. (2005) *J. Biol. Chem.* **280,** 31257–31266
8. Yang, H., Xie, W., Xue, X., Yang, K., Ma, J., Liang, W., Zhao, Q., Zhou, Z., Pei, D., Ziebuhr, J., Hilgenfeld, R., Yuen, K. Y., Wong, L., Gao, G., Chen, S., Chen, Z., Ma, D., Bartlam, M., and Rao, Z. (2005) *PLoS Biol.* **3,** e324
9. Lee, T.-W., Cherney, M. M., Huitema, C., Liu, J., James K. E., Powers, J. C., Eltis, L. D., and James, M. N. G. (2005) *J. Mol. Biol.* **353,** 1137–1151
10. Tan, J., Verschueren, K. H. G., Anand, K., Shen. J., Yang, M., Xu, Y., Rao, Z., Bigalke, J., Heisen, B., Mesters, J. R., Chen, K., Shen, X., Jiang, H., and Hilgenfeld, R. (2005) *J. Mol. Biol.* **354,** 25–40
11. Xu, T., Ooi, A., Lee, H.-C., Wilmouth, R., Liu, D. X., and Lescar, J. (2005) *Acta Crystallogr. F Struct. Biol. Crystalliz. Comm.* **61,** 964–966
12. Shi, J., Wei, Z., and Song J. (2004) *J. Biol. Chem.* **279,** 24765–24773
13. Fan, K., Wei, P., Feng, Q., Chen, S., Huang, C., Ma, L., Lai, B., Pei, J., Liu, Y., Chen, J., and Lai, L. (2004) *J. Biol. Chem.* **279,** 1637–1642
14. Chen, S., Chen, L., Tan, J., Chen, J., Du, L., Sun, T., Shen, J., Chen, K., Jiang, H., and Shen, X. (2005) *J. Biol. Chem.* **280,** 164–173
15. Kuang, W.-F., Chow, L.-P., Wu, M.-H., and Hwang, L.-H. (2005) *Biochem. Biophys. Res. Commun.* **331,** 1554–1559
16. Hsu, W.-C., Chang, H.-C., Chou, C.-Y., Tsai, F.-J., Lin, P.-I., and Chang, G.-G. (2005) *J. Biol. Chem.* **280,** 22741–22748
17. Chou, C.-Y., Chang, H.-C., Hsu, W.-C., Lin, T.-Z., Lin, C.-H., and Chang, G.-G. (2004) *Biochemistry* **43,** 14958–14970
18. Berendsen, H. J. C., van der Spoel, D., and van Drunen, A. R. (1995) *Comput. Phys. Commun.* **91,** 43–56
19. Lindahl, E., Hess, B., and van der Spoel, D. (2001) *J. Mol. Model* **7,** 306–317
20. Jorgensen, W. L., Maxwell, D. S., and Tirado-Rives, J. (1996) *J. Am. Chem. Soc.* **118,** 11225–11236
21. Jorgensen, W. L., Chandrasekhar, J., Madura, J. D., Impey, R. W., and Klein, M. L. (1983) *J. Chem. Phys.* **79,** 926–935
22. Nosé, S. (1984) *Mol. Phys.* **52,** 255–268
23. Parrinello, M., and Rahman, A. (1981) *J. Appl. Phys.* **52,** 7182–7190
24. Darden, T., York, D., and Pedersen, L. (1993) *J. Chem. Phys.* **98,** 10089–10092
25. Hess, B., Bekker, H., Berendsen, H. J. C., and Fraaije, J. G. E. M. (1997) *J. Comput. Chem.* **18,** 1463–1472
26. Neria, E., Fischer, S., and Karplus, M. (1996) *J. Chem. Phys.* **105,** 1902–1921
27. Brooks, B. R., Bruccoleri, R. E., Olafson, B. D., States, D. J., Swaminathan, S., and Karplus, M. (1983) *J. Comput. Chem.* **4,** 187–217
28. Huang, C., Wei, P., Fan, K., Liu, Y., and Lai, L. (2004) *Biochemistry,* **43,** 4568–4574
29. Wei, P., Fan, K., Chen, H., Ma, L., Huang, C., Tan, L., Xi, D., Li, C., Liu, Y., Cao, O., and Lai, L. (2006) *Biochem. Biophys. Res. Commun.* **339,** 865–872
30. McDonald, I. K., and Thornton, J. M. (1994) *J. Mol. Biol.* **238,** 777–793

Only One Protomer Is Active in the Dimer of SARS 3C-like Proteinase

Hao Chen, Ping Wei, Changkang Huang, Lei Tan, Ying Liu and Luhua Lai

J. Biol. Chem. 2006, 281:13894-13898.
doi: 10.1074/jbc.M510745200 originally published online March 24, 2006
